AD-A210 085

# Energy Transfer from High Power Pulselines to the Next Generation of PRS Loads

R.E. TERRY

*Plasma Radiation Branch*
*Plasma Physics Division*

F.L. COCHRAN

*Berkeley Research Associates*

DTIC
ELECTE
JUL 1 2 1989
D

June 15, 1989

89     7    11    090

# REPORT DOCUMENTATION PAGE

Form Approved
OMB No. 0704-0188

| 1a REPORT SECURITY CLASSIFICATION | 1b RESTRICTIVE MARKINGS |
|---|---|
| UNCLASSIFIED | |

| 2a. SECURITY CLASSIFICATION AUTHORITY | 3 DISTRIBUTION / AVAILABILITY OF REPORT |
|---|---|
| 2b. DECLASSIFICATION / DOWNGRADING SCHEDULE | Approved for public release; distribution unlimited. |

| 4. PERFORMING ORGANIZATION REPORT NUMBER(S) | 5 MONITORING ORGANIZATION REPORT NUMBER(S) |
|---|---|
| NRL Memorandum Report 6491 | |

| 6a. NAME OF PERFORMING ORGANIZATION | 6b OFFICE SYMBOL (If applicable) | 7a. NAME OF MONITORING ORGANIZATION |
|---|---|---|
| Naval Research Laboratory | Code 4720 | |

| 6c. ADDRESS (City, State, and ZIP Code) | 7b ADDRESS (City, State, and ZIP Code) |
|---|---|
| Washington, DC 20375-5000 | |

| 8a. NAME OF FUNDING / SPONSORING ORGANIZATION | 8b OFFICE SYMBOL (If applicable) | 9 PROCUREMENT INSTRUMENT IDENTIFICATION NUMBER |
|---|---|---|
| Defense Nuclear Agency | RAEV | |

| 8c. ADDRESS (City, State, and ZIP Code) | 10 SOURCE OF FUNDING NUMBERS | | | |
|---|---|---|---|---|
| | PROGRAM ELEMENT NO | PROJECT NO | TASK NO | WORK UNIT ACCESSION NO |
| | 62715H | | | DN880-191 |

11. TITLE (Include Security Classification)

Energy Transfer from High Power Pulselines to the Next Generation of PRS Loads

12 PERSONAL AUTHOR(S)
Terry, R.E. and Cochran,* F.L.

| 13a TYPE OF REPORT | 13b TIME COVERED | 14 DATE OF REPORT (Year, Month, Day) | 15 PAGE COUNT |
|---|---|---|---|
| Interim | FROM _____ TO _____ | 1989 June 15 | 29 |

16 SUPPLEMENTARY NOTATION
(See page ii)

| 17 | COSATI CODES | | 18 SUBJECT TERMS (Continue on reverse if necessary and identify by block number) |
|---|---|---|---|
| FIELD | GROUP | SUB-GROUP | Plasma radiation source      Inductive energy storage |
| | | | Saturn pulseline      Power flow |

19 ABSTRACT (Continue on reverse if necessary and identify by block number) •

The efficiency of energy transfer to model PRS loads on high power pulselines is investigated with a series of PRS models and a transmission line code.

| 20 DISTRIBUTION / AVAILABILITY OF ABSTRACT | 21 ABSTRACT SECURITY CLASSIFICATION |
|---|---|
| ☒ UNCLASSIFIED/UNLIMITED  ☐ SAME AS RPT  ☐ DTIC USERS | UNCLASSIFIED |

| 22a NAME OF RESPONSIBLE INDIVIDUAL | 22b TELEPHONE (Include Area Code) | 22c OFFICE SYMBOL |
|---|---|---|
| Dr. Jack Davis | (202) 7673278 | Code 4720 |

DD Form 1473, JUN 86          Previous editions are obsolete          SECURITY CLASSIFICATION OF THIS PAGE

S/N 0102-LF-014-6603

16. SUPPLEMENTARY NOTATION

*Berkeley Research Associates

# CONTENTS

# ENERGY TRANSFER FROM HIGH POWER PULSELINES
# TO THE NEXT GENERATION OF PRS LOADS

## I. Introduction

The design of more complex loads for Plasma Radiation Sources and the quest for ever higher simulator radiative yields and power levels require heretofore unexplored energy densities in the load region, perhaps as high as 1.50 $MJ/cm^3$. Quite apart from detailed design questions, there is some concern that these higher power and energy densities (delivered by "sub-Ohm" pulselines) cannot couple well to the PRS configurations used today or to even higher inductance designs that might be used in the future.

In this report we will examine the energy transfer to two PRS loads from generic pulselines of the Saturn class operating at the 8 $\rightarrow$ 15 $MA$ level. Saturn is nearly a 10x machine in terms of power flows and has recently been outfitted with PRS front end hardware; it is modeled in a subsequent section (III). A basic slug PRS model and an appropriate X-pinch model, derived from 2-D MHD simulations, are used.

The pulselines are modeled with a transmission line code, described in the next section (II). Apart from generalization to spacetime dependent line parameters (impedance, propagation speed, and damping), the solution technique is quite standard, robust, and accurate in its energy transfer characteristics. Even the simplest transmission line models of machines like Saturn provide the expected result – PRS loads will accommodate the line impedance and draw energy effectively. A more delicate question is that of loss mechanisms. This is left to future work.

In Section IV the coupling of pulsers like Saturn or the Falcon design (proposed by PI as a 10x device) to an X-pinch load is discussed. The particular load chosen is first modeled with the 2-D MHD code PRISM to exhibit the behavior we wish to exploit. The inductance history can then be used as a rough guide to the behavior

1

of such loads in Saturn or Falcon class machines.

Section V is devoted to a discussion of the results, conclusions and the implications for future efforts.

## II. Transmission Line Model

Existing transmission line models come in several variations. Within the MAGIC [2] program exist options for coupling transmission lines to a variety of 2-D simulation regions as well as the use of parallel and series junctions among lines. Within the BERTHA [3] package exists a broad spectrum of line elements on which waves are propagated without distortion by summation of forward and backward disturbances. In any study of energy coupling to the time dependent PRS one must join the transmission line to varying load parameters $Z(t)$, $L(R(t))$, allow for space time varying line parameters, and also drive the system with a fixed initial energy. No existing transmission line code offered ready access to all these capabilities, so a simple implementation of the 1-D telegrapher's equations has been written to treat such problems.

Resolving the continuous transmission line into discrete units of inductance per unit length ($L'$) in series with the load and capacitance per unit length ($C'$) in parallel with the load, the telegrapher's equations can be written in the dimensionless forms

$$^{n+1}V_j = {}^nV_j - \alpha Z_j \left( {}^{n+1/2}I_j - {}^{n+1/2}I_{j-1} \right),$$

$$(\mathcal{D}_- \, {}^{n+1/2}I)_j = (\mathcal{D}_+ \, {}^{n-1/2}I)_j - \frac{\alpha}{Z_j} \left( {}^nV_{j+1} - {}^nV_j \right),$$

where the matrix operator

$$\mathcal{D}_\pm = (\mathcal{I} \pm \gamma \alpha \, \nabla^2)_{ij} \ ,$$

2

introduces an adjustable damping parameter

$$\gamma \approx \frac{1}{8} \propto \frac{k_{Nyq}}{k_{damp}}$$

which controls the dispersion of the method at high wavenumber. By damping out the large wave number components, the tendency of these difference equations to propagate higher wavenumbers more slowly is mitigated and low wavenumber pulse shapes are then transmitted with low harmonic distortion. Here the parameter $\alpha = ch_t/h_x$ is the Courant number, and $Z_j$ can be spatially and temporally variable.

At the boundaries the damping is set to zero, the combination of exterior circuit elements and the local currents on the transmission line then fixes the time advanced currents and voltages through:

$$^{n+1/2}I_o = {}^{n-1/2}I_o - \frac{\alpha}{Z_o} \left( {}^nV_1 - {}^nV_o \right) ,$$

$$^{n+1/2}I_J = {}^{n-1/2}I_J - \frac{\alpha}{Z_J} \left( {}^nV_{J+1} - {}^nV_J \right) ,$$

$$^nV_o = \frac{Z_o\tau V_s(t) + L_o^{\,n}V_1}{Z_o\tau + L_o} ,$$

$$^nV_{J+1} = \frac{\tau Z_J\,{}^nI_J Z_L(t) + L(R)^nV_J}{\tau Z_J + L(R)} ,$$

where the time derivative of current has been eliminated in favor of the appropriate voltage differences and $\tau$ is the delay interval of a single element, viz. $\tau = h_x/c$. The source voltage $V_s(t)$ can be derived through a variety of methods, e.g., a fixed waveform, or a computed capacitive discharge. The load is characterized by a time dependent inductance $L(R,t)$ and resistance $Z_L(t)$. Here $R$ denotes the load radius, and $\dot{R}$ must be included in the load resistance.

For a PRS load a wide variety[4-8] of simple models has been used in this context. Each choice made in configuring the load model has consequences for the calcu-

lation as a whole which are substantially impossible to generalize and which produce a variety of transmission line responses. In order to set the proper damping parameter and thus to calibrate the basic method, a simpler problem is appropriate.

If the input voltage is specified as a Gaussian pulse with a variable width relative to the transmission line time and the load is a fixed impedance equal to that of the transmission line, then the ideal response is a distortion free propagation of the Gaussian pulse. Given an upper limit to the wavenumber which can be resolved by the difference equations, the damping added must attenuate the higher wavenumber components enough to prevent the "shedding" of aphysically slow "wake" disturbances, but not so large as to interfere with an accurate portrayal of the energy transport in the line.

The use of a $\gamma$ value of about 0.125, corresponding to a damping wavenumber at about 4 times the Nyquist wavenumber, offers a reasonable compromise in this tradeoff. With an overall energy conservation error of $5.15 \cdot 10^{-4}$, Figure 1 shows the result of propagating a 50 ns pulse over a 22.5 ns length of $1/8 \, \Omega$ line into a matched load. The Gaussian envelope at the output is essentially self-similar to that at the input, being scaled down slightly due to the attenuation in the method. There are no reflections at the interface for the matchload at any part of the wavenumber spectrum.

Figure 1



MATCHED LOAD WAVEFORMS ON (0,125) [ns]

4
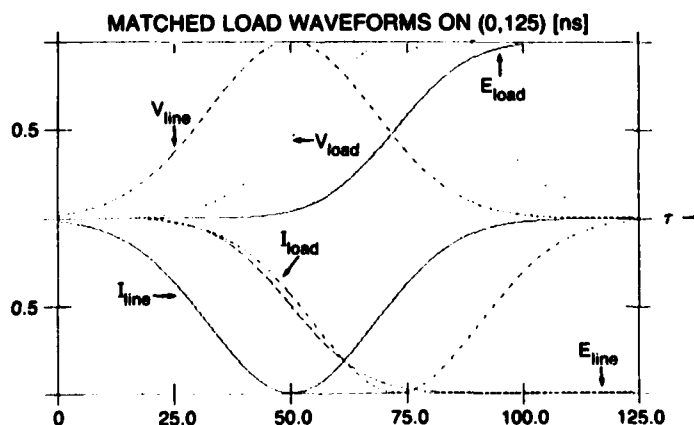
## III. Application to Saturn

A simple model of the Saturn machine at SNL can be formed from three elements: a pulse source, a long transmission line section equivalent to the four parallel water lines which bring the power down to a radius of 1 m, and a short transmission line delivering the power to the load region which, in the PRS mode, offers an initial inductance of 5→10 nH.

In practice the transition between the two lines is a post-hole convolute, while the shorter line offers a fixed impedance for only part of the path to the load, after which it becomes a simple radial line, viz. $Z \propto 1/R$. The details of the Marx bank will be ignored here – let it be abstracted to a single fast pulse (4.4 MV and 50 ns $\frac{1}{c}$ width) in series with a small resistance (0.12 Ω). Likewise, the convolute details will be ignored as well, it is abstracted to a discrete jump in impedance to 3.3 Ω, up from the 1/4 Ω of the parallel water lines.

In terms of detailed experimental support such minutiae as these are important, but in this examination of gross power coupling they will not matter and they are modeled [9] elsewhere. The primary quest here is the energy coupling characteristics of Saturn class machines to various PRS configurations. The simplest adequate model can therefore be abstracted to the following transmission line problem.

Figure 2
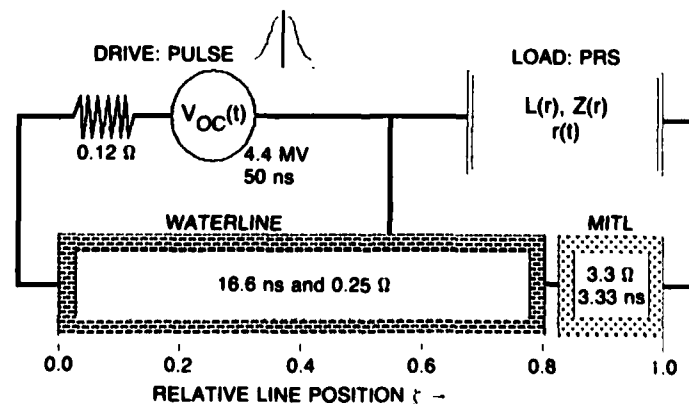
To drive 10x machine currents to a PRS load in $\approx 100ns$ requires $V_{oc} \approx 4MV$ on the driver pulse, and a forward energy fluence of $\approx 1MJ$ into the waterline.

As a further benchmark test of the transmission line code, a similar problem was run on the BERTHA package[10] with an 1/8 $\Omega$ line impedance and a fixed load impedance of 3/8 $\Omega$. Both calculations agree to a few percent in the timing of various reflections, the timing of current reversals and in the peak values of the voltage and current waveforms (at the input to the line and at the load).

### Slug PRS Model

The early phase of implosion presumes a snowplow like compression of the full load mass. Even though such an idealization is not likely to be completely accurate, for several reasons, the most serious consequence is a shift of the optimum mass point for radiation yield. The most important variable in the calculation of the run down is the motional impedance. I have shown elsewhere[11] that a variety of details in the current penetration and radiation physics still allows a rough adherence to the familiar snowplow velocity scaling with electric field – either for a slug or for a fully resolved 1-D load model. As a consequence the slug model will capture the proper trends in generator/load coupling even if the point by point comparisons may differ somewhat from the actual experiment.

Employing a series resistance and inductance for the slug load, both time varying as determined by the load radius, the governing equations for the run down phase become:

$$\ddot{R} = -\frac{I^2}{\mu c^2 R} \; ,$$

$$L(R) = \frac{2d}{c^2} \ln(\frac{R_{wall}}{R}) \; ,$$

$$Z_L = Z_o - \frac{2d}{c^2} \frac{\dot{R}}{R} \; ,$$

with $Z_o$ fixed, $d$ the AK gap, $R_{wall}$ the radius of the return current path in the load region, $\mu$ the load mass per unit length, and $Z_o$ the average impedance of the plasma, viz. $Z_o = \frac{\eta d}{\pi R^2}$. The choice $\eta$ is reasonably taken to produce a $Z_o$ in the $10m\Omega$ range at early times. Coupling the relations to the transmission line solver is accomplished by calculating $R$, $\dot{R}$, $Z_L$ and $L(R)$ at each timestep. The energy absorbed in the load region is then $\int^t dt_1 \ V_L(t_1) I_L(t_1) dt_1$ as inferred from the line solution.

As the run-down terminates the plasma load should ideally undergo a non-adiabatic stagnation and convert the input energy to radiation. The final state of the load plasma is almost never very simple, but a rough average picture is to model it as a Bennet equilibrium pinch. The Bennet current figures as a central notion in oscillatory MHD solutions as well, so an order of magnitude sort of model can set the final impedance at a fixed final radius, $R_{min}$. If the pinch temperature is eliminated in favor of the current, one finds that the Bennet profile offers an impedance

$$Z_L = 1.109 \cdot 10^9 \left( \frac{d \ \mu^{3/2}}{R_{min}^2 I_{kA}^3} \right) \ [\Omega] \ ,$$

where $I_{kA}$ is in units of $kA$, $R_{min}$ is chosen initially, and the motional impedance is assumed to vanish.

### Energy Coupling and Stagnation Radius

The radial structure of a PRS load will generally have a substantial effect on the radius of the current path at stagnation. Efficient radiative loss can deepen the implosion by perhaps a factor of 10; turbulent enhancement of plasma resistivity can spread the current channel and increase the final radius. While the final radius is therefore not a "free" parameter is any sense, it is a very relevant measure of the

7

*implosion quality. Moreover, the logarithmic singularity in the load inductance as $R_{min} \to 0$ makes this parameter appear to be important for energy transfer. While the values of $R_{min}$ examined here are a bit smaller than those observed in practice, the machine behavior expected if very small radii are achieved is a worthwhile target in a study of this kind.*

*On the transmission line, the load implosion and stagnation appears as a backward propagating pulse – lowering the current and increasing the voltage. As the load samples larger inductance values due to smaller $R_{min}$ this "downward" current pulse turns into a full current reversal. The larger $R_{min}$ values thus imply a mild power reflection back up the line, while the smaller values imply a rather effective rejection of power by the load.*

*Figure 3(a,b) ..................................... Figure 4(a,b)*
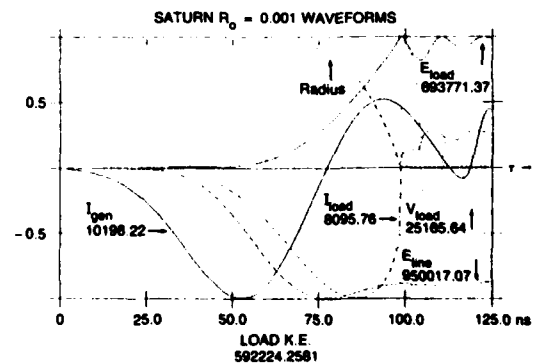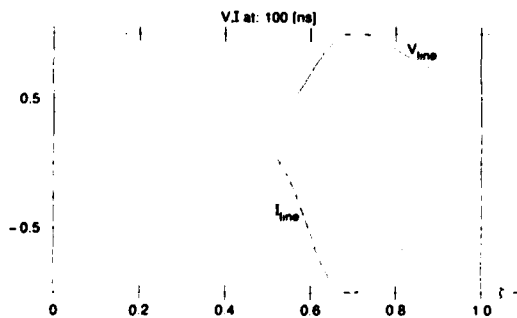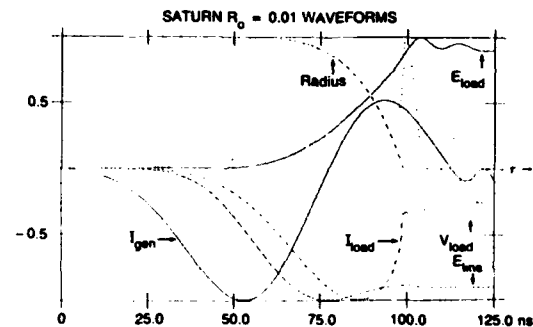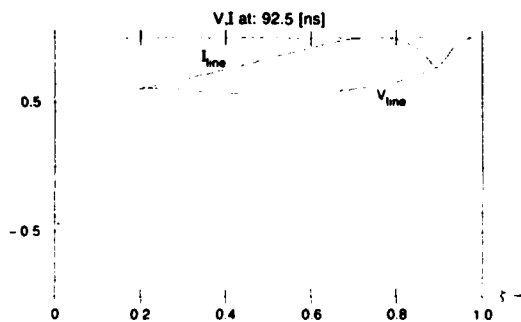
In Figure 3 are two snapshots of the reflection in a Saturn calculation, one at $R_{min} = 0.01cm$, the other at $R_{min} = 0.001cm$. In Figure 4 are shown the drive and load I and V waveforms, as well as the energy into the line and into the load. The load radius is also plotted. All such runs as these were done with a load mass of 100 $\mu g/cm$ and produced a peak load current $\approx 8MA$. The mass is such that implosion occurs at $\approx 100ns$ and the reflected power is therefore unable to go up and back before the run ends at 125 ns.

Under the assumptions of this PRS model, when the load reverses the current the energy leaves the load region because all the energy is in the fields around it. The real behavior would likely be more dissipative and not allow as much energy release to the line. It is therefore reasonable to compare the energy coupled to the load region to that coupled to a 1/4 $\Omega$ matched load in the constant 125 ns interval. The results are summarized in the following Figure 5, where the efficiencies of overall energy transfer – $\eta_L = E_{Load}/E_{match}$ – and transfer to load kinetic energy – $\eta_T = T_{PRS}/E_{match}$ are plotted.

Figure 5

## SATURN ENERGY TRANSFER EFFICIENCY



9
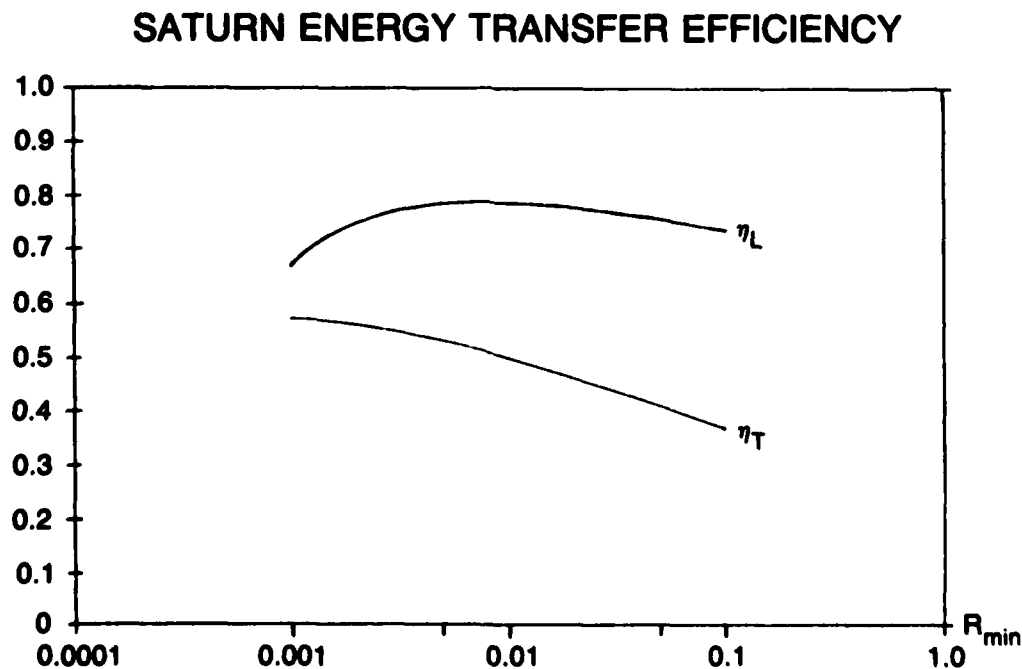
## IV. X-pinches in Saturn and Falcon

The X-pinch load has heretofore been configured[12,13] as two or more crossed wires in a diode gap. The central motivation being to focus more of the machine power on a smaller volume of plasma in hopes of exciting more K-shell radiation. A different quest for the X-pinch can also be contrived – the production of a "mini-diode" plasma state which will make effective use of nonthermal electron populations in exciting K-shell radiation.

In order to produce such a "mini-diode" one can exploit the sausage instability through judicious mass loading. Using the simple scaling law for the implosion time pointed out by Apruzese [7], a constraint of fixed time from different radii imposes a particular mass per unit length on any extended load configuration –

$$\mu_o = 1.1972 \cdot 10^3 (\frac{\tau_o I_p}{R_o})^2 \; [\mu g/cm] \; ,$$

such that, for a fixed run down time $\tau_o$ to a peak current $I_p$, a figure of revolution $R_o(Z)$ must be mass loaded as above in order to implode synchronously at all axial locations. In Figure 6 are shown the density contours of such a load exactly as it was represented in the 2-D MHD code PRISM. The conical portion helps to keep the inductance lower at early times, while the cylindrical segment near the midplane is allowed a greater or lesser rundown length to provide a store of kinetic energy upon stagnation.

Figure 6



10
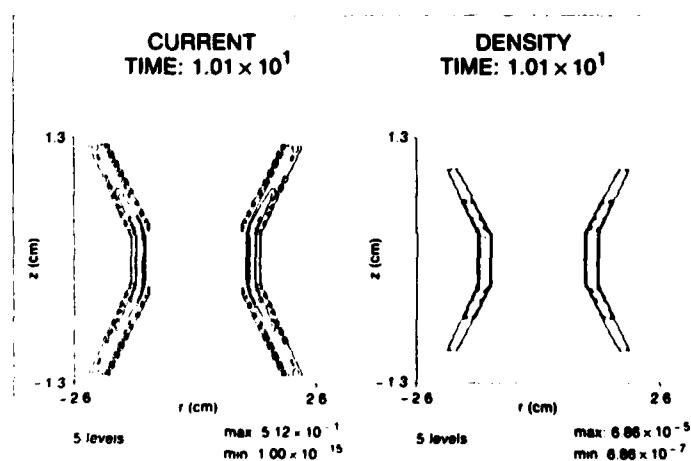
This load configuration was imploded through the use of a current ramp which rose linearly to 3 MA in 100 ns. While there is certainly some detailed structure produced during the rundown, the dominant kinematics is precisely as inferred from the 0-D scaling law. By 90 ns (c.f. Figure 7), the conical portion has run down a bit faster and two density peaks have appeared about the midplane. Some material

Figure 7,8,9
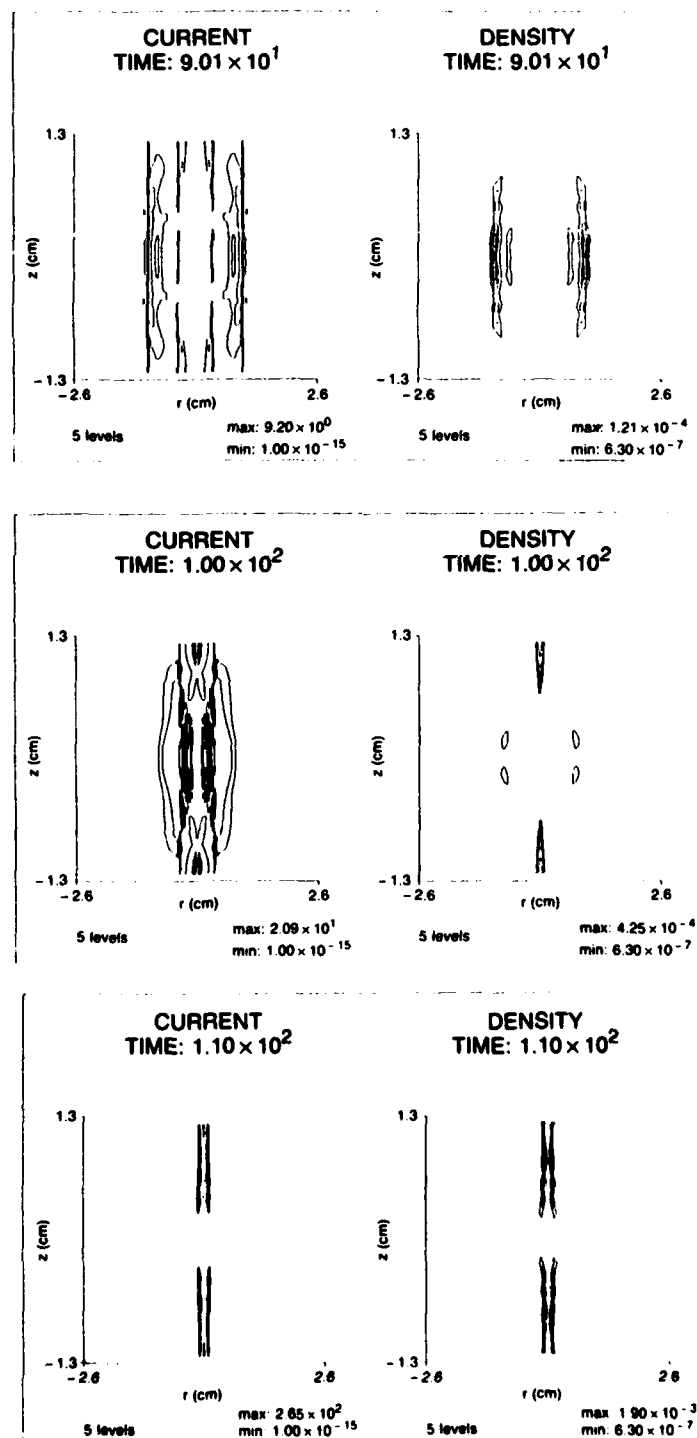
has been pushed ahead near the midplane due to magnetic field penetration and the resulting spallation when the shock emerged into the interior.

Upon stagnation at about 100 ns the load dynamics does reflect the structural details impressed during the rundown. The sausage instability goes rapidly to a saturated state – the current density is shown to leave the necked down region – and the originally cylindrical segment is bifurcated, c.f. Figure 8. The split state persists for some 10 ns more through the end of the simulation, Figure 9.

Here "stagnation" connotes the arrival of material on axis, the history of the density there is shown in Figure 10. The overall load design has thus produced its intended result – there is a density cavity of nearly two orders of magnitude near the midplane over which the diode voltage must be dropped!

Figure 10



12
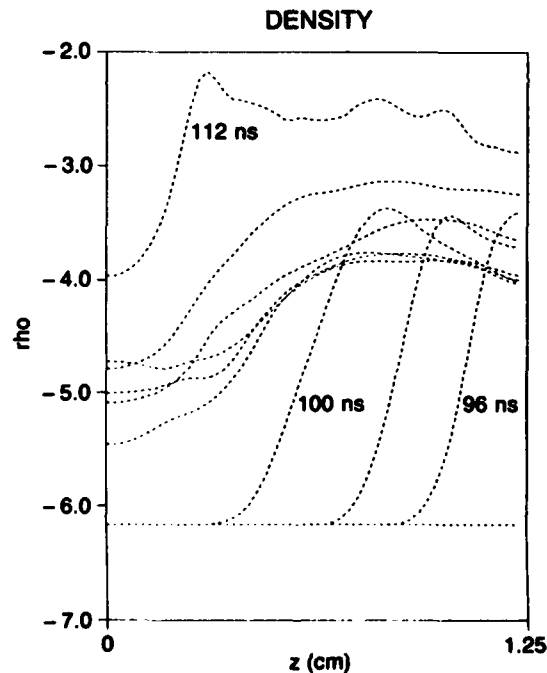
We leave to future work the assessment of runaway electron populations in such a load. For now, in the context of a 10x machine, it is reasonable to examine the energy delivery to such a load when it is characterized by a time dependent inductance and the implied motional impedance. When the evolution in 2-D shown above is reduced to an inductance history one finds the behavior shown in Figure 11. There is shown the inductance added by the imploding X-pinch and a similar (in mass, radius and current) slug implosion.

For the model to work with the transmission line code this function must be mapped into the familiar triad $[\ L(R), Z_L(R,\dot{R})$, and $R(t)\ ]$. The radius we use is a current weighted one, viz. derived from the volume exterior to the current channel.

Figure 11

## INDUCTANCE OF THE X-PINCH



13
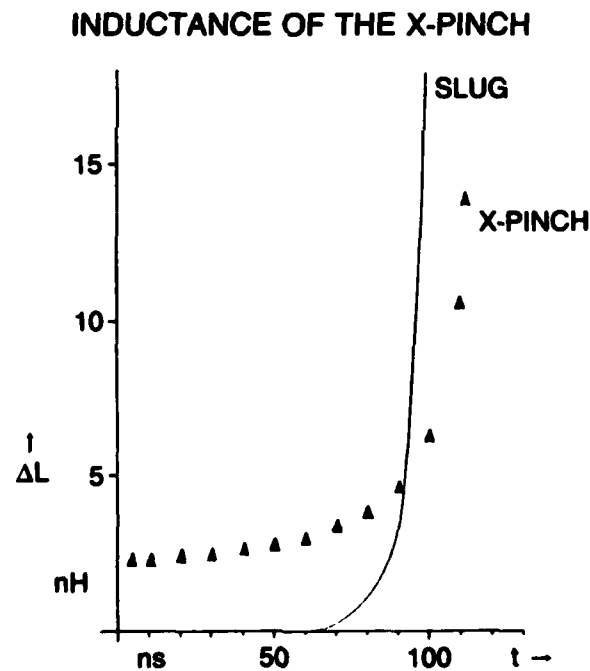
## Saturn X-pinch

When the X-pinch model is used in place of the slug in the same machine simulation of Saturn detailed above, the energy transfer is somewhat lower due to the lack of enough motional impedance to draw energy from the line. The overall waveforms are shown in Figure 12, and the inductive "notch" is much less pronounced. The inferred efficiency $\eta_L$ is 0.45, and the peak load current is 8.3MA.

*Figure 12*

**SATURN XP WAVEFORMS**

Radius

$E_{load}$

0.5

$\tau \rightarrow$

$V_{load}$

-0.5

$I_{gen}$

$I_{load}$

$E_{line}$

0      25.0      50.0      75.0      100.0      125.0 ns
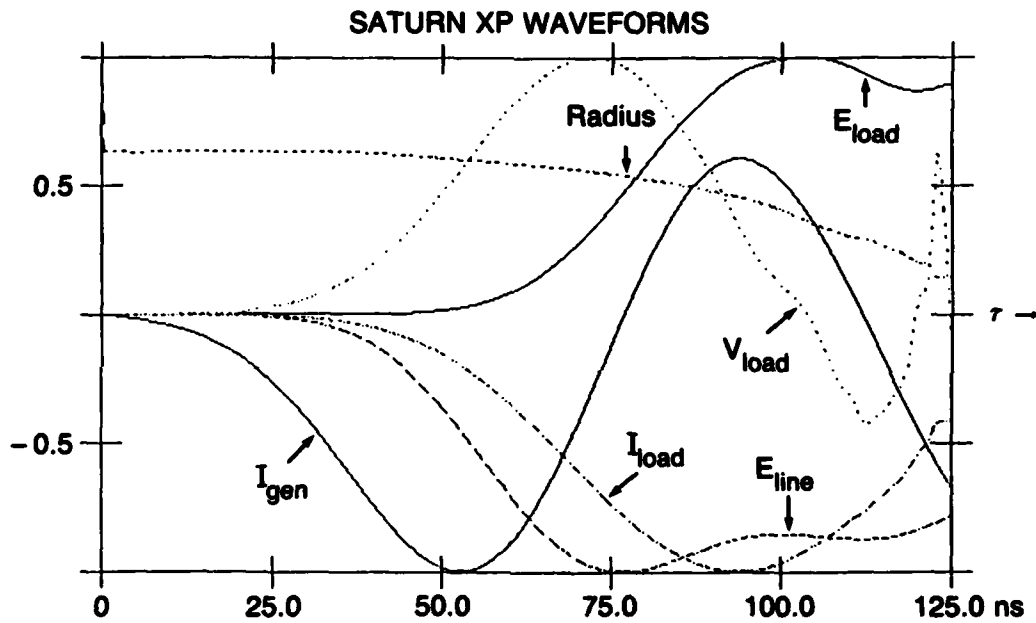
### Falcon X-pinch

Since the Falcon design is concerned with an inductive storage device, the circuit and transmission line model changes slightly. In a Falcon 10x machine eight inductive energy stores (IES) are switched together into a single MITL at about a meter radius which then must converge the power to a PRS load. The IES modules would have a quarter period of $\approx 1.27\mu s$, each being charged to perhaps 720 kV and using a storage inductor of about 150 nH in vacuum prior to the opening switch. A reasonably generous estimate of the inductance downstream of the opening switch (before the PRS load implodes) is perhaps 18 nH. Thus, working from a meter radius or 3 ns, the final transmission line impedance is 6 $\Omega$.

When all eight modules are connected and switched out near peak current one has some 30 MA available to drive the final line and PRS. Not all of this current is expected in the imploding load, most of the energy will be dissipated in the opening switch or left in the inductance of the store and final transmission line. However, even with all these sinks the final energy to an imploding load is easily competitive with Saturn. If, for example, the Falcon opening switch were to achieve an $\dot{R} \approx 0.05\Omega/ns$, the energy delivery efficiency to a slug load ($\eta_L$), relative to the original stored energy, is $\approx 0.46$ – in the same range that Saturn achieves into a slug load. This efficiency is computed over the same time interval, $[0,125]ns$, and decays with slower opening rates. If the X-pinch load is examined at the same opening rate, the efficiency decays to $\approx 0.36$. The peak current expected in the Falcon X-pinch would be $\approx 17.0 MA$, again comparable to Saturn.

### V. Conclusions

All the experience to date with this transmission line and load model indicates that for all of the generic machine designs presently contemplated for the 10x ma-

15

*chine, for all the likely domains of load stagnation radius, one can state two results with some confidence.*

- *The front end inductance of a PRS load per se is not a problem for energy coupling, provided this inductance remains in the range $\leq 20nH$.*

- *The gas puff PRS load on Saturn should draw at least $8 \to 10\ MA$ in the present configuration.*

*The observed behavior[14] on Saturn – 10 MA into gas puffs and 12.5 MA into short circuit loads – is quite nicely in line with this prediction.*

*Furthermore, all the experience to date with the more complex X-pinch load design indicates that (i.) it represents a very credible PRS concept in terms of energy coupling and (ii.) it should be quite compatible with the presently contemplated 10x machine designs. The model we have discussed here will be refined further by 2D MHD studies to include the role of runaway electron populations in the energy budget and to optimize the load dynamics.*

*More general problems, involving loss mechanisms in MITL segments, can be readily addressed by the method and some initial work is already underway.*

### References

1. *Theoretical and Experimental Comparison of GAMBLE II Argon Gas Puff Experiments, J. W. Thornhill, et. al., NVOO Proceedings, to be published, 1988.*

2. *MAGIC Users Manual, B. Goplen, et. al., MRC/WDC-R-126.*

3. *D. D. Hinshelwood, NRL Memo Rep. 5185, 1983, "BERTHA - A Versatile Transmission Line and Circuit Code".*

4. *D. Mosher, NRL Memo Rep. 3687, 1978, "Coupling of Imploding-Plasma Loads to High-Power Generators".*

5. *R. E. Terry and J. U. Guillory, "Development and Exploration of the Core-Corona Model of Imploding Plasma Loads," DNA Report 5234F, 1980.*

6. *J. U. Guillory and R. E. Terry, "Modeling of Imploded Annular Plasmas," DNA Report 6152F, 1982.*

7. *J. P. Apruzese and J. Davis, NRL Memo Rep. 5406, 1984, "K-Shell Yield Scaling Law for Conventional PRS Loads".*

8. *S. W. McDonald and P. F. Ottinger, NRL Memo Rep. 5785, 1986, "Modeling and Simulation of an Imploding Plasma Radiation Source".*

9. *P.Corcoran,et. al., Pulse Sciences Rep. PSI-FR390-05, Oct 1988, "Sandia Double Post Hole Convolute Puff Diode, Final Electrical and Mechanical Design"*

10. *A. E. Robson, private communication.*

11. *R. E. Terry, et. al., Bull. APS, 1984, "Velocity Scaling of the Radiatively Dominated Z-Pinch".*

12. *K. G. Whitney, J. Davis, and N. R. Pereira, NRL Memo Rep. 5970, 1987, "New Load Design Concepts for Z-Pinches."*

13. *N. Loter, et. al. and J. Davis, et. al., Maxwell Laboratory Rep. MLR-3017,*
*"Advanced Wire Experiments on Blackjack 5", 1988.*

14. *P. Spence, R. Spielman, private communication.*

# DISTRIBUTION LIST

Assistant to the Secretary of Defense          1 copy
Atomic Energy
Washington, D.C.  20301
Attn:  Executive Assistant

Director
Defense Nuclear Agency
Washington, D.C.  20305
Attn:  DDST          1 copy
      TITL          4 copies
      RAEV          1 copy
      STVI          1 copy

Commander          1 copy
Field Command
Defense Nuclear Agency
Kirtland AFB, New Mexico  87115
Attn:  FCPR

Chief          1 copy
Field Command, Livermore Division
Department of Defense
Post Office Box 808
Livermore, California  94550
Attn:  FCPRL

Director          1 copy
Joint Strat TGT Planning Staff
Offutt AFB
Omaha, Nebraska  68113
Attn:  JLKS

Undersecretary  of Defense          1 copy
for RSCH and ENGRG
Department of Defense
Washington, D.C.  20301
Attn:  Strategic and Space Systems (OS)

Deputy Chief of Staff for RSCH DEV and ACQ          1 copy
Department of the Army
Washington, D.C.  20301
Attn:  DAMA-CSS-N

Commander          1 copy each
Harry Diamond Laboratories
Department of the Army
2800 Powder Mill Road
Adelphi, Maryland  20783
Attn:  DELHD-N-NP
      DELHD-R J. Rosado
      DELHD-TA-L (Tech. Lib.)

U.S. Army Missile Command                          3 copies
Redstone Scientific Information Center
Attn: DRSMI-RPRD(Documents)
Redstone Arsenal, Alabama  35809


Commander                                          1 copy
U.S. Army Nuclear and Chemical Agency
7500 Backlick Road
Building 2073
Springfield, Virginia  22150
Attn: Library


Commander                                          1 copy
Naval Intelligence Support Center
4301 Suitland Road, Bldg. 5
Washington, D.C.  20390
Attn: NISC-45


Commander                                          1 copy
Naval Weapons Center
China Lake, California  93555
Attn: Code 233 (Tech. Lib.)


Officer in Charge                                  1 copy each
White Oak Laboratory
Naval Surface Weapons Center
Silver Spring, Maryland  20910
Attn: Code R40
      Code F31


Air Force Weapons Laboratory                       1 copy each
Kirtland AFB, New Mexico  87117
Attn: SUL
      CA
      APL
      Lt. Col Generosa


Deputy Chief of Staff                              1 copy
Research, Development and Accounting
Department of the Air Force
Washington, D.C.  20330
Attn: AFRDQSM


Commander                                          1 copy
U.S. Army Test and Evaluation Command
Aberdeen Proving Ground, Maryland  21005
Attn: DRSTE-EL

AVCO Research and Systems Group                1 copy
201 Lowell Street
Wilminton, Massachusetts  01887
Attn:  Library A830

BDM Corporation                                1 copy
7915 Jones Branch Drive
McLean, Virginia  22101
Attn:  Corporate Library

Berkeley Research Associates                   1 copy
Post Office Box 983
Berkeley, California  94701
Attn:  Dr. Joseph Workman

Berkeley Research Associates                   1 copy each
Post Office Box 852
5532 Hempstead Way
Springfield, Virginia   22151
Attn:  Dr. Joseph Orens

Boeing Company                                 1 Copy
Post Office Box 3707
Seattle, Washington  98134
Attn:  Aerospace Library

The Dikewood Corporation                       1 copy
1613 University Blvd., N.E.
Albuquerque, New Mexico  87110
Attn:  L. Wayne Davis

General Electric Company - Tempo              1 Copy
Center for Advanced Studies
816 State Street
Post Office Drawer QQ
Santa Barbara, California  93102
Attn:  DASIAC

Institute for Defense Analyses                1 copy
1801 N. Beauregard Street
Alexandria, Virginia  22311
Attn:  Classified Library

IRT Corporation                               1 copy
Post Office Box 81087
San Diego, California  92138
Attn:  R. Mertz

JAYCOR                                        1 copy
1608 Spring Hill Road
Vienna, Virginia  22180
Attn:  R. Sullivan

```
JAYCOR                                              1 copy
11011 Forreyane Road
Post Office Box 85154
San Diego, California  92138
Attn:  E. Venaas
       F. Felbar


KAMAN Sciences Corporation                          1 copy each
Post Office Box 7463
Colorado Springs, Colorado  80933
Attn:  Library


Lawrence Livermore National Laboratory              1 copy each
University of California
Post Office Box 808
Livermore, California  94550
Attn:  DOC CDN for 94550
       DOC DCN for L-47 L. Wouters
       DOC CDN for Tech. Infor. Dept. Lib.


Lockheed Missiles and Space Company, Inc.           1 copy each
Post Office Box 504
Sunnyvale, California  94086
Attn:  S. Taimlty
       J.D. Weisner


Lockheed Missiles and Space Company, Inc.           1 copy
3251 Hanover Street
Palo Alto, California  94304
Attn:  J. Perez


Maxwell Laboratory, Inc.                            1 copy ea.
9244 Balboa Avenue
San Diego, California  92123
Attn:  A. Kolb
       M. Montgomery
       J. Shannon


McDonnell Douglas Corporation                       1 copy
5301 Bolsa Avenue
Huntington Beach, California  92647
Attn:  S. Schneider


Mission Research Corporation                        1 copy each
Post Office Drawer 719
Santa Barbara, California  93102
Attn:  C. Longmire
       W. Hart
```

Mission Research Corporation-San Diego                1 copy
5434 Ruffin Road
San Diego, California  92123
Attn:  Victor J. Van Lint

Northrop Corporation                                  1 copy
Northrop Research & Technology Center
1 Research Park
Palos Verdes Peninsula, California  90274

Physics International Company                         1 copy
2700 Merced Street
San Leandro, California  94577
Attn:  M. Krishnan
       C. Gilman
       S. Wong

R and D Associates                                    1 copy each
Post Office Box 9695
Marina Del Rey, California  90291
Attn:  Library

Sandia National Laboratories                          1 copy each
Post Office Box 5800
Albuquereque, New Mexico  87115
Attn:  Doc Con For 3141
       D. McDaniel
       P. VanDevender
       K.  Matzen, Code 4247

Science Applications, Inc.                            1 copy
Post Office Box 2351
La Jolla, California    92038
Attn:  R. Beyster

Spectra Technol, Inc.,                               1 copy
2755 Northup Way
Bellevue, Washington  98004
Attn:  Alan Hoffman

Spire Corporation                                    1 copy
Post Office Box D
Bedford, Massachusetts 07130
Attn:  R. Little

S-CUBED                                              1 copy
Post Office Box 1620
La Jolla, California  92038
Attn:  A. Wilson

Director                                              1 copy each
Strategic Defense Initiative Organization
Pentagon   20301-7100
Attn:   DE    Lt. Col Richard Gullickson/DEO
        IST   Dr. Dwight Duston

Texas Tech University                                 1 copy
Post Office Box 5404
North College Station
Lubbock, Texas   79417
Attn:   T. Simpson

TRW Defense and Space Systems Group                   1 copy
One Space Park
Redondo Beach, California   90278
Attn:   Technical Information Center

Naval Research Laboratory
Plasma Radiation Branch
Washington, D.C.   20375
Code   4720 - 50 copies
       4700 - 26 copies
       2628 - 22 copies